

Towards an Effective Synthesis of Difunctionalized Heptacyclo[6.6.0.0^{2,6}.0^{3,13}.0^{4,11}.0^{5,9}.0^{10,14}]tetradecane: Ligand Effects on the Cage Assembly and Selective C–H Arylation Reactions

Xavier Marset,^a Martí Recort-Fornals,^a Malkaye Kpante,^b Adam Zieliński,^a Christopher Golz,^a Lawrence M. Wolf,^{b,*} and Manuel Alcarazo^{a,*}

^a Institut für Organische und Biomolekulare Chemie
Georg August Universität Göttingen
Tammannstr 2, 37077 Göttingen, Germany
Tel.: +49 (0) 0551/39-21711
E-mail: manuel.alcarazo@chemie.uni-goettingen.de

^b Department of Chemistry
University of Massachusetts Lowell
Lowell, Massachusetts 01854, United States
Tel.: +1 (978) 934-5877
E-mail: Lawrence_Wolf@uml.edu

Manuscript received: April 19, 2021; Revised manuscript received: May 17, 2021;
Version of record online: ■■■, ■■■



Supporting information for this article is available on the WWW under <https://doi.org/10.1002/adsc.202100481>

© 2021 The Authors. Advanced Synthesis & Catalysis published by Wiley-VCH GmbH. This is an open access article under the terms of the Creative Commons Attribution Non-Commercial License, which permits use, distribution and reproduction in any medium, provided the original work is properly cited and is not used for commercial purposes.

Abstract: A series of strong π -acceptor polyfluorinated and dicationic chelating phosphines have been synthesized and evaluated in the Rh-catalysed dimerization of norbornadiene (NBD) into its thermodynamically more stable dimer, heptacyclo[6.6.0.0^{2,6}.0^{3,13}.0^{4,11}.0^{5,9}.0^{10,14}] tetradecane (HCTD). While dicationic ligands direct the dimerization towards HCTD, by the use of neutral polyfluorinated ancillary ligands *endo-endo*-heptacyclo[8.4.0.0^{2,12}.0^{3,8}.0^{4,6}.0^{5,9}.0^{11,13}]tetradecane (BINOR-S) is selectively obtained. In addition, a selective Pd-catalysed arylation at position C8 of the HCTD framework is achieved by the use of a picolylamide directing group previously attached at C1. Theoretical calculations have been performed to understand the origin of that regioselectivity.

Keywords: Phosphane ligands; C–H Activation; Palladium; Rhodium; Density functional calculations

Introduction

The selective functionalization of adamantane (**1**) and diamantane (**2**) has attracted enormous attention due to the numerous applications that these derivatives have found in areas as diverse as material science^[1] or medicine.^[2] Thus, a number of adamantane derived amines are approved drugs that display potent antiviral **3–6**, anti-diabetes **7–8** or anti-acne **9** activity among others.^[3] Moreover, the adamantyl structure has also been introduced into the structure of already known pharmaceuticals to enhance their lipophilicity and

improve their pharmacokinetics.^[2b,4] Selected examples of such drugs are shown in Figure 1A.

The available methodologies enabling the introduction of an initial substituent into the naked diamandoid scaffolds typically follow mechanisms that proceed via radical or carbocationic intermediates, a circumstance that severely restricts the incoming of the first functionalization to one (or several) of the bridgehead methine positions.^[5] Regioselective functionalization of two neighbouring carbons, a methine and a methylene units, are possible when a former substituent already present in the adamantane framework is able to assist the second C–H activation acting as directing

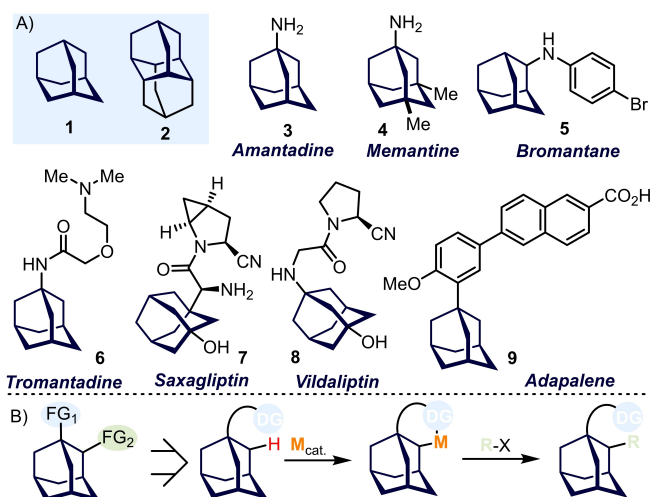
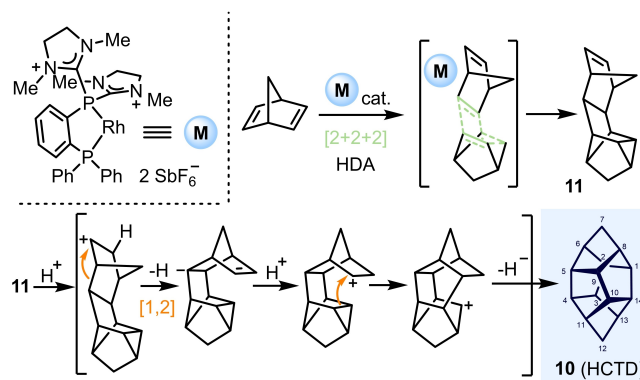


Figure 1. a) Selected examples of adamantane-containing therapeutics and b) Typical strategies for the synthesis of 1,2-disubstituted adamantanes via C–H functionalization.

group in typically a metal catalysed process (Figure 1B).^[6] Despite this, the number of protocols already established to access 1,2-disubstituted adamantane derivatives is comparatively quite reduced.^[7]

Even more scarce are the examples in which the adjacent di-functionalization of heptacyclo [6.6.0.0^{2,6}.0^{3,13}.0^{4,11}.0^{5,9}.0^{10,14}] tetradecane (HCTD, **10**), the *D*_{2d}-symmetric isomer of **2** in which all carbons are part of five-membered rings, has been achieved. The routes available proceed through oxidative opening of the cage and without exception deliver product mixtures and marginal yields. The scope of products attainable is also extremely limited.^[8] No directing group-based strategy seems to have been employed in this issue. The reason for this probably lies in the fact that a practical multi-gram synthesis of **10** has remained a challenge for decades.^[9] Only two protocols are known to deliver **10** in significant amount and with high selectivity; one based on Ru-catalysis,^[10] and a second one recently reported by our group.^[11] We used a Rh catalyst bearing a dicationic ancillary phosphine to promote the initial dimerization of norbornadiene (NBD) into its *exo-cis-endo* dimer **11** following a *homo*-Diels-Alder cyclization mechanism. Subsequently, the cage closure towards **10** is promoted by Brønsted acid catalysis (Scheme 1).

With a view toward enabling the further development of HCTD chemistry, we tackle herein two important aspects. First, we have evaluated the effect of a series of newly prepared strong acceptor bidentate ligands, cationic and neutral ones, on the dimerization process of NBD into **11**. Additionally, the possibility of synthesizing disubstituted HCTDs making use of a directing group strategy has been addressed. A major challenge here is to achieve selectivity during the C–H



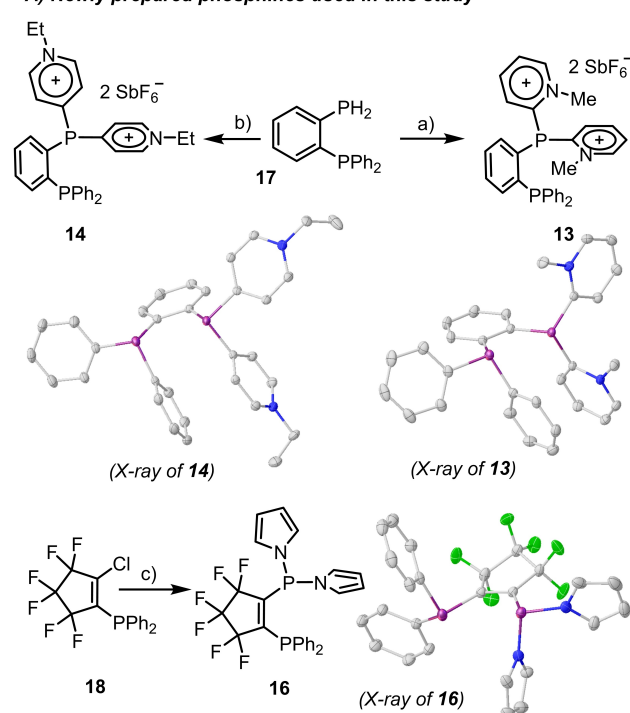
Scheme 1. Synthesis of **10** via Rh-catalysed dimerization of NBD to **11** and subsequent Brønsted acid promoted cage closure.

activation step. Note that once the directing group is installed at the most reactive C1 position, all three neighboring moieties are non-equivalent but comparably reactive methines, which indeed deliver different regioisomeric products after the functionalization event. Building up on the accumulated knowledge for adamantane substrates,^[7] we describe herein the use of a bidentate picolyl amide as directing group, which successfully deals with the foregoing selectivity problem in a Pd-catalysed C–H arylation process.

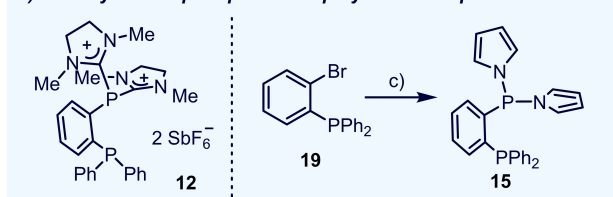
Results and Discussion

At the outset of this investigation, the preparation of phosphines **13**–**16** was conceived. As in the case of known **12**, they all share a neutral −PPh₂ fragment but differ in the linker that connects the two phosphine units, and the nature of the electron withdrawing groups attached to the second phosphorous atom. Ligands **13** and **14** formally exchange the dimethylimidazolium moieties of **12** by *o*- and *p*-pyridinium groups, respectively. In **15** the same role is taken by 1-pyrrolyl substituents. Finally, in **16** a hexafluorocyclopentenyl linker connects the two phosphorus atoms (Scheme 2a). Compounds **13** and **14** were obtained in 48% and 39% yields by reaction of primary diphosphine **17** with 1-methyl-2-chloropyridinium tetrafluoroborate or 1-ethyl-4-iodopyridinium tetrafluoroborate, respectively; followed by anion exchange with NaSbF₆ (Scheme 2a). The formation of the desired ligands was first suggested by NMR spectroscopy. The ³¹P-NMR spectra of both compounds consist of two doublets with identical coupling (δ_p = −12.5 (P2), −23.8 (P1) ppm., *J*_{pp} = 182.0 Hz for **13**; and δ_p = −10.9 (P2), −12.2 (P1) ppm., *J*_{pp} = 151.8 Hz for **14**), which are attributed with certainty to the −PPh₂ and [−P(py)₂]⁺ moieties, respectively. This initial structural assignment was later confirmed by X-ray crystallography;

A) Newly prepared phosphines used in this study



B) Already known phosphines employed for comparison



Scheme 2. Synthesis and molecular structures of the newly prepared ligands **13–15** and **16**; X-ray structures of **13**, **14** and **16**. Hydrogen atoms, anions and solvent molecules were removed for clarity; ellipsoids are set at 50% probability.^[12] Reagents and conditions: a) 1-methyl-2-chloropyridinium tetrafluoroborate (2 equiv.), Et₃N (2 equiv.), THF, 60 °C; then NaSbF₆ (excess) in CH₃CN; **13**, 48%; b) 1-ethyl-4-iodopyridinium tetrafluoroborate (2 equiv.), Et₃N (2 equiv.), THF, 60 °C; then NaSbF₆ (excess) in CH₃CN; **14**, 39%; c) *n*-BuLi, CIP(1-pyrrolyl)₂, **15**, 67%; **16**, 74%.^[12]

the ORTEP diagrams of **13** and **14** are also depicted in Scheme 2.

Diphosphine **16** has been prepared in 74% yield by lithiation of **18** and subsequent reaction with (pyrrolyl)₂PCl,^[13] following an analogous protocol to the one described for the synthesis of **15** starting from *o*-(bromophenyl)diphenylphosphine **19**.^[14] X-ray crystallography has also confirmed the atom connectivity in **16** (Scheme 2).

The global donor ability of **13**, **14** and **16** was estimated through comparative analysis of the CO stretching frequencies of Mo complexes **20–22** with those already reported for **23–25** (Figure 2).^[14,15] The

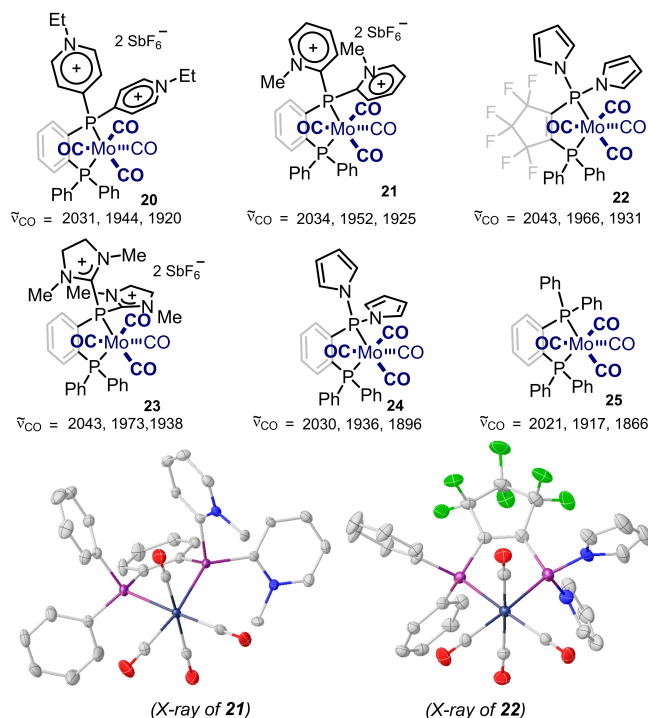
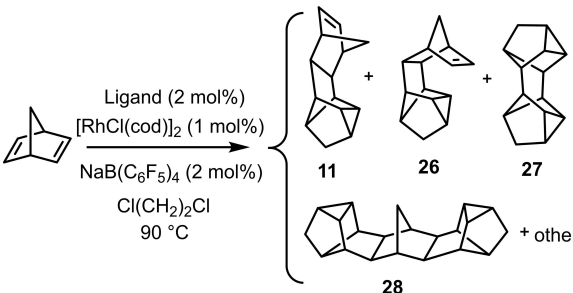


Figure 2. Evaluation of the donor abilities of **13**, **14** and **16**, and X-ray structures of **21** and **22**. Hydrogen atoms, anions and solvent molecules were removed for clarity; ellipsoids are set at 50% probability. Wavenumbers in cm^{−1}.^[12]

ν_{CO} values recorded for dicationic **20** (2031, 1944, 1920 cm^{−1}) and **21** (2034, 1952, 1925 cm^{−1}) are slightly lower than those observed for **23** (2043, 1973, 1938 cm^{−1}) suggesting that the imidazolium unit is able to induce a stronger acceptor character in the adjacent phosphorus than 2- or 4-pyridinium moieties. By virtue of its polyfluorinated backbone **16** is certainly an exceptionally strong π -acceptor ligand as well; however, comparison of the ν_{CO} stretching frequencies of **22** with those of **23**, indicates that **16** is not able to overtake **12** in that regard. Hence, all three new auxiliary ligands prepared seem to be slightly weaker π -acceptors than **12**.

Once prepared, the performance of ligands **12–16** on the dimerization of NBD was evaluated. The standard conditions employed were those previously optimized for **12**: NBD (0.2 M in Cl(CH₂)₂Cl), 90 °C, 2 mol% of ligand and 1 mol% of [RhCl(cod)]₂. NaB(C₆F₅)₄ (2 mol%) was added as additive to improve the solubility.^[16]

The results obtained are compiled in Table 1. Ligand **13** performed poorly, mainly NBD polymers were produced together with some minor quantities of HCTD (2.5%). We believe that this result derives from the partial hydrolysis of **13** with adventitious water present in the reaction mixture. The protons liberated through this process might ultimately be responsible

Table 1. Ligand effects on the Rh-catalyzed dimerization of NBD.


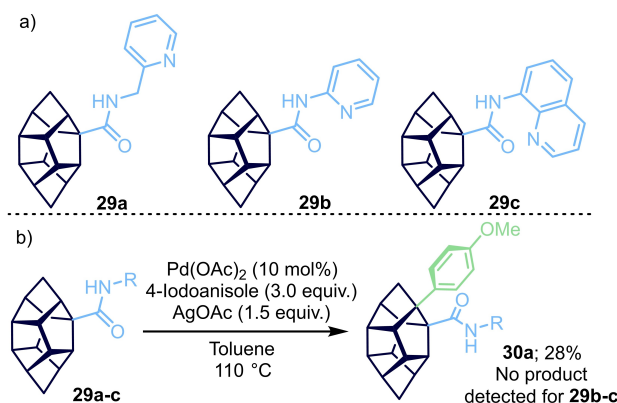
Entry ^[a]	Ligand	Ratio 11:26:27:28:other (%)	Conv.(%)
1	12	86:10:0:1:3	97
2	13	polymers	64
3	14	55:8:0:35:2	71
4	15	18:1:42:26:13	60
5	16	0:0:89:9:2	67

^[a] Experiments carried out with an initial NBD concentration of 0.2 M.

for the uncontrolled NBD polymerization (entry 2). Contrarily, **14** preferentially directs the dimerization of NBD to **11**. Conversions however are not as high as those obtained with **12**, and significant amounts of undesired trimer **28** are formed (entry 3). Ligand **15** promotes the unselective formation of many NBD dimers, being *endo-endo*-heptacyclo [8.4.0.0^{2,12}.0^{3,8}.0^{4,6}.0^{5,9}.0^{11,13}]tetradecane (BINOR-S, **27**) the major isolated product (entry 4). Finally, under the aforementioned catalytic conditions, ligand **16** leads the dimerization towards **27** in nearly an exclusive manner although NBD consumption was never complete (entry 5). From these studies we conclude that all strong π -acceptor ligands tested facilitate NBD dimerization, but cationic ones seem to be essential to obtain dimer **11** with high conversion. The reasons why **15** and **16** preferentially direct the dimerization process to the formation of BINOR-S **27** still remains unclear, steric factors may also play a role.

At this stage the possibility of preparing disubstituted HCTDs via a directed C–H functionalization strategy was addressed. Based on the existing reports on amide-directed Pd-catalyzed C–H arylation of adamantane structures,^[7] compounds **29a–c** were identified as promising model substrates. They were synthesized from the corresponding acid chloride, which was obtained by modification of an already described synthetic protocol (Scheme 3a and Supporting Information).^[17]

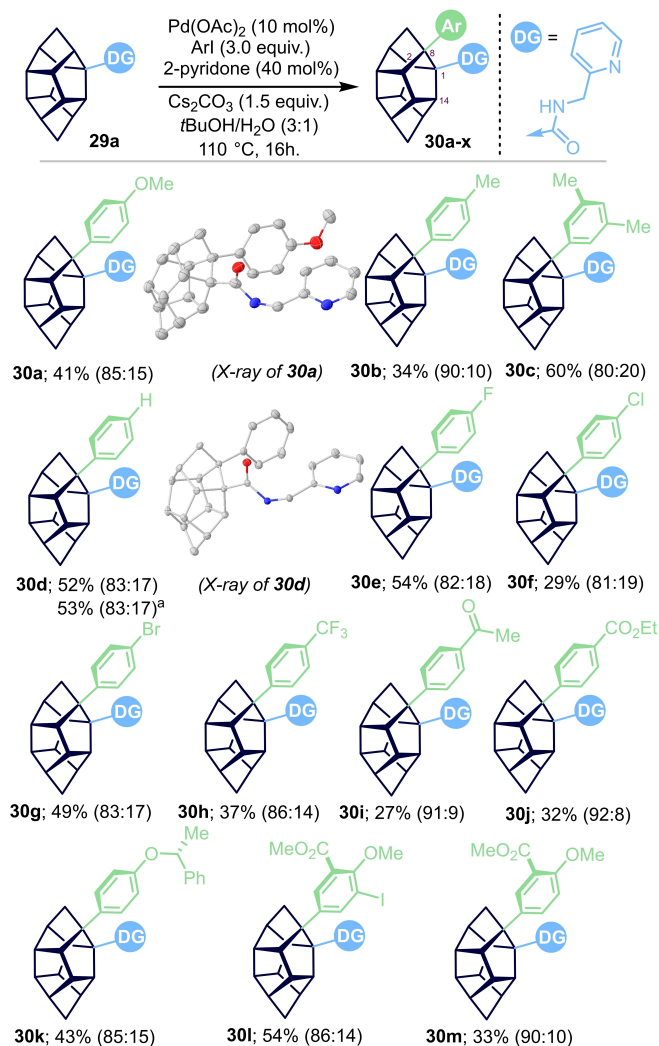
Initially, the reaction was conducted using Pd(OAc)₂ (10 mol%) as catalyst, AgOAc (1.5 equiv.) as base and halogen scavenger, and 4-iodoanisole as the arylating reagent in toluene at 110 °C. Under these conditions only substrate **29a** delivered the desired

**Scheme 3.** a) Screening of directing groups, and b) model reaction.

product **30a**, and was therefore used for further optimization (Scheme 3b). A survey of different bases, solvents, temperatures and other additives were screened; a detailed list of all these experiments is shown in the Supplementary Information. It is worth mentioning that the use of 2-pyridone (40 mol%) was essential to improve the conversion towards **30**, without this additive it never reached more than 40%; the use of 2-pyridones substituted with electron-withdrawing groups did not improved that result.^[18] Finally, we also found that the solvent mixture *t*BuOH:H₂O (3:1) is also ideal in this case to avoid the formation of diarylated products.^[19] In summary, the optimal conditions found are the following: Pd(OAc)₂ (10 mol%), ArI (3.0 equiv.), Cs₂CO₃ (1.5 equiv.), 2-pyridone (40 mol%), in *t*BuOH:H₂O (3:1) at 110 °C; which were further used to evaluate the scope of the arylation reaction (Scheme 4). Aryl rings decorated with both, electron donating or electron withdrawing substituents are well tolerated in this transformation producing the desired products; *para*- and *meta*-substituents are tolerated but not *ortho*- ones. Yields are moderate in all cases.

Given the intricate structure of **29a**, which contains eleven methine units, three of them in the direct neighborhood of the directing amide group; the determination of the actual position that is preferentially arylated is not evident by conventional NMR-analysis. It was only through X-ray analyses of crystals of products **30a** and **30d** that the substitution pattern in **30a–m** could be unambiguously established.

The aryl groups occupy position 8- of the HCTD cage (Scheme 4). The origin for this selectivity is studied in detail in the theoretical section, but the X-ray structure of **29a** is already quite instructive in this regard. The position that gets functionalized is the most pyramidalized one (sum of the three basal C–C–C angles around C8 is 308.2°, 313.6° for C2 and 316.1° for C14). Further derivatization of the products

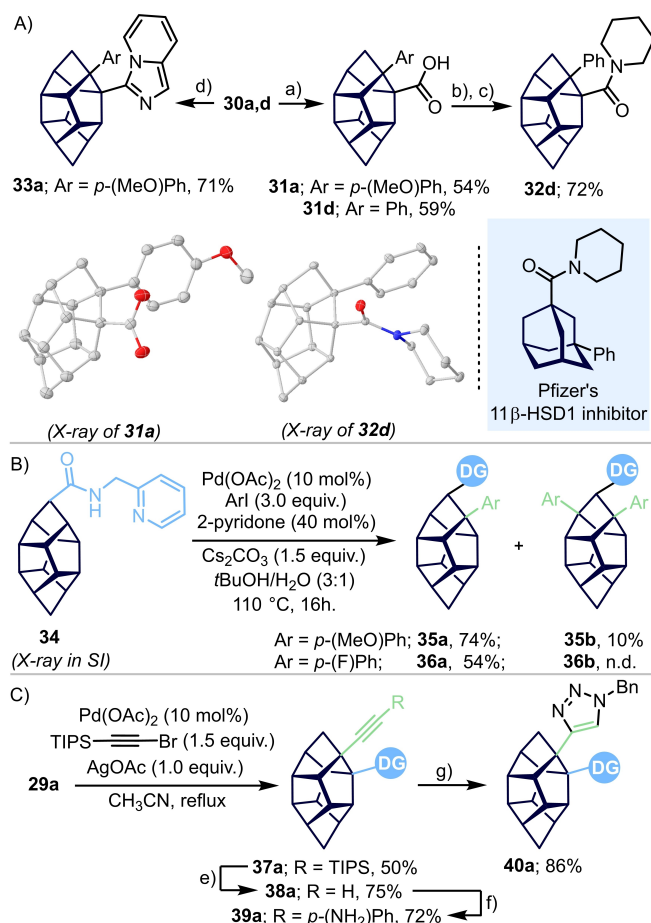


Scheme 4. Scope of the arylation reaction. Yields are of isolated monoarylated products; C8:C14 arylation ratios in crude reaction mixtures were determined by ¹H-NMR analysis and are shown in parenthesis. ^aReaction performed on 1 mmol scale.^[12]

obtained has also been attempted. For example, the amide moiety of **30 a,d** can be hydrolyzed under strong acidic conditions delivering the corresponding free acids **31 a,d**.^[6d] Subsequently, compound **31 d** has been further transformed into piperidine amide **32 d**, which is structurally related to Pfizer's non-steroid 11 β -HSD1 inhibitor (Scheme 5).^[20] Imidazo[1,5*a*]pyridine derivative **33 a** was obtained via Tf₂O-promoted intramolecular cyclisation of the directing group.

Installation of the amide directing group in position 7- of the HCTD skeleton is also possible. In that case under the reaction conditions already developed, the C–H arylation also takes place at C8; diarylation however, is also detected (Scheme 5B).

Even more interestingly is the fact that other C–H functionalization reactions can be performed as well,



Scheme 5. A) Derivatization of **30 a–d**; B) difunctionalization of HCTDs with amide group at position 7; C) C–H alkynylation of **29 a**; n.d. = not detected. Reagents and conditions: a) H₂SO₄ (40%), *p*-xylene, 130 °C, 24 h.; b) SO₂Cl₂, reflux, 3 h.; c) piperidine (1.5 equiv.), Et₃N (1.5 equiv.), DCM, r.t.; d) Tf₂O, DCM, 35 °C; e) TBAF (1.2 equiv.), THF, r.t.; f) 4-iodoaniline (2.0 equiv.), (PPh₃)₂PdCl₂ (5 mol%), CuI (10 mol%), Et₃N (3.0 equiv.), DMF, r.t.; g) BnN₃ (1.0 equiv.), sodium ascorbate (0.5 equiv.), CuSO₄ (10 mol%), CHCl₃/H₂O (4:1), r.t.^[12]

under similar reaction conditions. For example, employing bromoalkynes as electrophilic partner, the C–H alkynylation of **29 a** takes place to deliver **37 a**,^[21] which subsequently after silyl group deprotection serves as a versatile synthetic intermediate (Scheme 5C).

In order to shed some light on the reaction mechanism with some focus on the regioselectivity of the C–H functionalization process, theoretical calculations at the level M06/def2-TZVPPD//B3LYP–D3/def2-SVP level of density functional theory were performed.^[22] The resulting predicted profile displays parallels with prior studies into the usage of 2-pyridone as mediating C–H bond activation, however the regioselectivity question here requires independent investigation.^[23] The profile begins with deprotonated

2-pyridone already coordinated to palladium through the O- and N-atoms. A C–H bond from the HCTD skeleton exchanges with the oxygen of 2-pyridone for a Pd coordination site giving rise to an agostic interaction in **INT0** (Figure 3). There is a small preference for C8–H coordination over the C14–H and C2–H bonds, which persists and widens in the subsequent C–H activation **TS1** with an increased preference for C8–H activation over C14–H or C2–H by ca. 2 and 4 kcal mol^{−1}, respectively. This is discussed in detail below. The pathways for C8–H and C14–H functionalization are further pursued to the final product. Following a concerted metalation deprotonation (CMD) mechanism^[24] **INT1** is formed, which then undergoes ligand exchange between 2-pyridone and iodobenzene to form **INT2**. Subsequent oxidative addition through **TS2** leads to the Pd(IV)-containing **INT3** with a barrier height of 19.5 kcal mol^{−1} from **INT1** for C8–H and 22.5 for C14–H. Lastly, rate limiting reductive elimination from the Pd(IV) generates a difunctionalized cage still coordinated to a Pd(II) species, which releases the product and reenters the catalytic cycle. The rate determining reaction barrier is predicted to be 23.9 kcal mol^{−1} from **INT1** to **TS3** for C8–H, which can be reasonably surmounted at the elevated temperatures used, and 29.6 kcal mol^{−1} for C14–H. Our calculations predict that from **INT1**, the barrier for surmounting **TS3** is slightly higher than reversion to the reactant, indicating a competition between the C–H activation and reductive elimination

as the selectivity determining steps. Alternatively, the iodide in **INT3** could undergo ligand exchange with an acetate which leads to a slightly lower barrier of 23.4 kcal mol^{−1} for the reductive elimination, with a lower predicted enthalpy for **TS3**_{OAc} compared to **TS1** (See SI). Hence, we arrive at the conclusion that reductive elimination is rate determining while C–H activation is likely selectivity determining with partial reversibility.

This reaction profile fits with the experimentally determined first order dependence of the reaction rate with respect to the concentrations of Pd catalyst and the aryl iodide, and also with the zero-order observed with respect to the amide substrate (See the Supporting Information). Additionally, incorporation of deuterium at C8 of the HCTD cage was detected when amide **29a** was subjected to the standard reaction conditions using *t*BuOD/D₂O as solvent system (19% deuterium incorporation after 16 h.). This result indicates that the C–H palladation step is likely reversible in this transformation.

The regioselective preference for C8–H activation was investigated using a non-covalent interaction analysis in the competing transition states, as well as an NBO analysis on the agostic complexes. An analysis of the agostic complexes provides some insight into the activation without bias in the competing transition states from differing extents of molecular distortion. Inspection of the total donation of the adjacent σ_{C-C} bonds to the C8–H σ^*_{C-H} reveals a greater

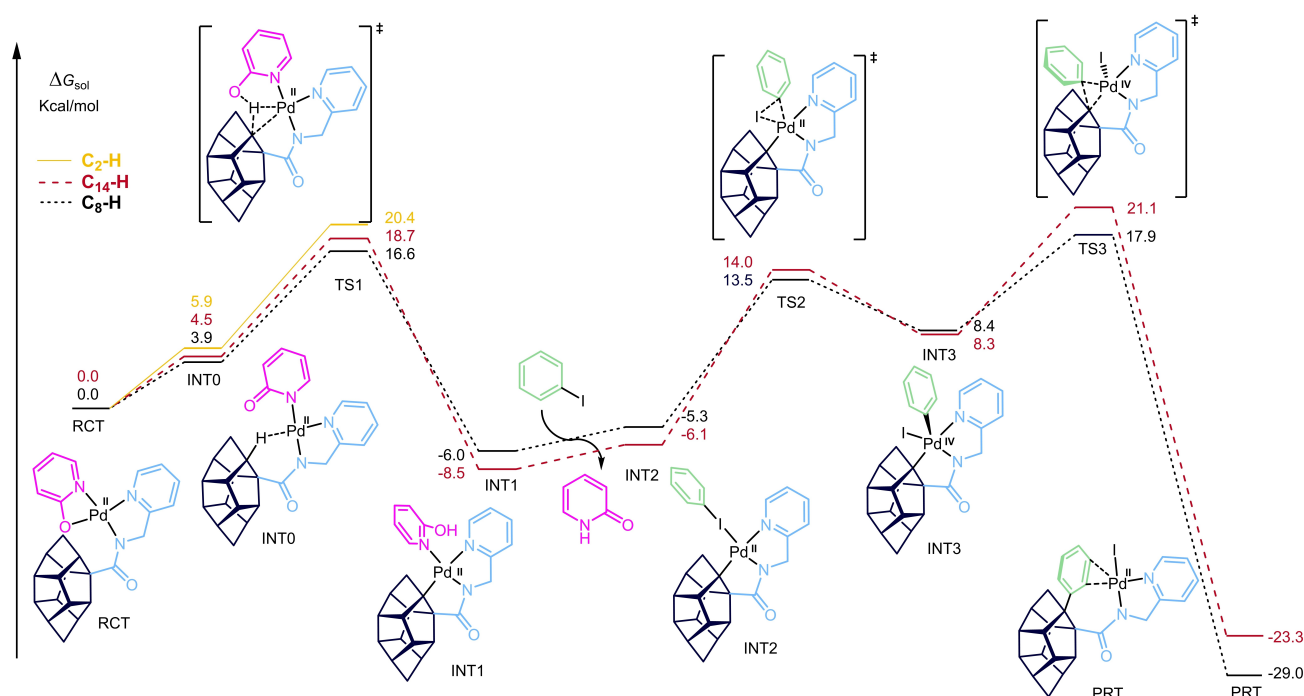


Figure 3. Gibbs free-energy profile computed at the M06(MeOH)/def2-TZVPP/B3LYP-D3/def2-SVP level of DFT for the C–H arylation reaction.

interaction by ca. 2 kcal/mol than analogous donor-acceptor interactions in the C₁₄-H and C2-H cases (Figure 4). The C8-H $\sigma^*_{\text{C-H}}$ in **INTO**_{C8-H} undergoes additional donor-acceptor interactions with the oxygen lone pairs of the pyridone ligand. These combined interactions lead to enhanced C–H bond weakening in **INTO**_{C8-H} relative to the isomeric C–H bonds with weaker relevant donor-acceptor interactions. These interactions culminate in a greater donation from the C8-H $\sigma_{\text{C-H}}$ to the Pd. The energetic separation in **TS1** for C8-H relative to C14-H and C2-H widens further as a result of developing steric interactions between the cage and the pyridone ligand not present in **TS1**_{C8-H}. The unfavourable interaction with the cage is manifest in the steric contour labelled as S1 not present in **TS1**_{C8-H}. **TS1**_{C2-H} is further destabilized by the steric interaction S2 representing a gauche like interaction between a methylene of the cage with amide group. The steric interaction S1 also serves to distort the CMD cyclic TS disrupting the necessary electronic reorganization.

Conclusion

The synthesis of a new set of polyfluorinated and dicationic π -acceptor bidentate phosphines is presented, their electronic properties are evaluated and their performance as ancillary ligands on the Rh-catalysed dimerization of NBD is studied. Unfortunately, none of the newly prepared phosphines is more efficient than **12** for this process. Additionally, we have developed a Pd(II) catalysed protocol for the regioselective arylation of the unactivated C8(*sp*³)-H bond of HCTD employing 2-picoylamide as directing group. The reaction follows a CMD like mechanism facilitated by 2-pyridone and the regioselectivity can be rationalized by a combination of enhanced C–H σ interactions with the metal center favouring the C8-H

isomer and unfavourable steric interactions with the cage in the formation of the minor C14-H isomer. This approach, which can also be extended to alkynylation reactions, represents the first example of directed C–H functionalization applied to the HCTD scaffold.

Experimental Section

General procedure for the Pd-catalyzed C–H arylation of HCTD. Compound **29a** (32 mg, 0.10 mmol), Pd(OAc)₂ (2.2 mg, 10 μ mol), Cs₂CO₃ (49 mg, 0.15 mmol), 2-pyridone (3.8 mg, 40 μ mol) and the respective aryl iodide (0.30 mmol) were placed in a microwave vial equipped with a stirring bar. *tert*-BuOH (0.75 mL) and H₂O (0.25 mL) were added, the vial was sealed under air atmosphere and heated at 110 °C for 16 h. Once the vial was cooled to room temperature, the crude mixture was diluted with EtOAc and filtered through a short pad of celite. The mixture was concentrated *in vacuo* and the desired products were isolated by column chromatography.

Compound **30a** was obtained according to general procedure in as a white solid (17 mg., 41% yield); m.p.=108–110 °C (EtOAc). *R*_f = 0.33 (hexane:acetone=3:2) ¹H NMR (CDCl₃, 400 MHz): δ 8.40 (d, *J*=5.0 Hz, 1H), 7.49 (td, *J*=7.7, 1.8 Hz, 1H), 7.20–7.12 (m, 2H), 7.09 (dd, *J*=7.6, 4.8 Hz, 1H), 6.74 (d, *J*=7.8 Hz, 1H), 6.73–6.65 (m, 2H), 6.25 (t, *J*=5.2 Hz, 1H), 4.32–4.18 (m, 2H), 3.69 (s, 3H), 3.21–3.17 (m, 1H), 2.94–2.79 (m, 3H), 2.79–2.55 (m, 7H), 2.19 (dd, *J*=10.4, 1.5 Hz, 1H), 2.00–1.86 (m, 2H). ¹³C NMR (CDCl₃, 101 MHz): δ 175.1, 158.0, 157.1, 148.9, 136.5, 134.8, 127.9, 122.0, 121.7, 113.6, 73.8, 69.6, 61.0, 60.5, 56.9, 55.4, 55.2, 53.9, 53.6, 52.6, 51.3, 51.0, 50.0, 46.6, 44.7, 42.9. HRMS calcd. for C₂₈H₂₉N₂O₂⁺ (M + H)⁺: 425.2224, found: 425.2223. IR (neat, cm^{−1}): 2943, 2863, 1636, 1511, 1435, 1245, 1181, 1035, 731.

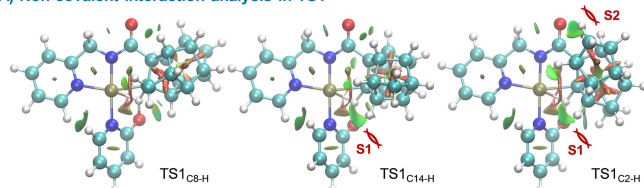
Acknowledgements

Support from the Deutsche Forschungsgemeinschaft through the projects AL 1348/8-2 and INST 186/1237-1 is gratefully acknowledged. X. M. thanks the Generalitat Valenciana (Spain) for a post-doctoral scholarship (APOSTD/2020/235). We also thank Martin Simon (University of Göttingen) for support with HPLC analyses and the members of our NMR and MS departments for excellent service.

References

- [1] For selected recent contributions see: a) F. Zou, H. Chen, S. Fua, S. Chen, *RSC Adv.* **2018**, *8*, 25584–25591; b) A. Kovalenko, C. Yumusak, P. Heinrichova, S. Stritesky, L. Fekete, M. Vala, M. Weiter, N. S. Sariciftci, J. Krajcovic, *J. Mater. Chem. C* **2017**, *5*, 4716–4723; c) K. Zhang, L. Wang, Y. Liang, S. Yang, J. Liang, F. Cheng, J. Chen, *Synth. Met.* **2012**, *162*, 490–496.
- [2] a) A. Štimac, M. Šekutor, K. Mlinarić-Majerski, L. Frkanec, R. Frkanec, *Molecules* **2017**, *22*, 297; b) L. Wanka, K. Iqbal, P. R. Schreiner, *Chem. Rev.* **2013**, *113*, 3516–3604; c) G. Lamoureux, G. Artavia, *Current. Med.*

A) Non-covalent interaction analysis in **TS1**



B) NBO analysis in agostic complex

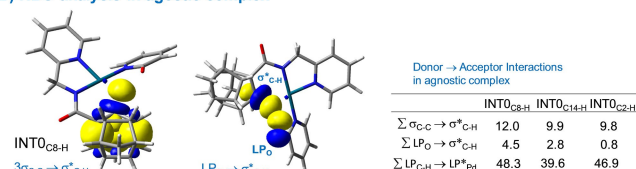



Figure 4. a) NCI plots highlighting unfavorable van der Waals interactions. b) NBO analysis of relevant donor-acceptor interactions.

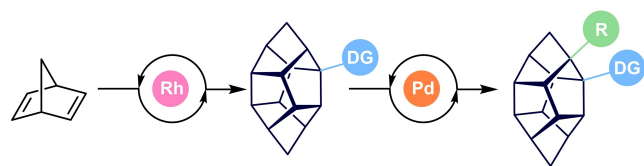
- Chem.* **2010**, *17*, 2967–2978; d) V. Y. Kovtun, V. M. Plakhotnik, *Pharm. Chem. J.* **1987**, *21*, 555–563.
- [3] a) M. Mikhaylova, J. Vakhitova, R. Yamidanov, M. Salimgareeva, S. Seredenin, T. Behnisch, *Neuropharmacology* **2007**, *53*, 601–608; b) A. Scherm, D. Peteri, DE 1941218 A **1971**; c) R. R. Grunert, J. W. McGahen, W. L. Davies, *Virology* **1965**, *26*, 262–269; d) W. L. Davies, R. R. Grunert, R. F. Haff, J. W. McGahen, E. M. Neumayer, M. Paulshock, J. C. Watts, T. R. Wood, E. C. Hermann, C. E. Hoffmann, *Science* **1964**, *144*, 862–863.
- [4] J. Liu, D. Obando, V. liao, T. Lifa, R. Codd, *Eur. J. Med. Chem.* **2011**, *46*, 1949–1963.
- [5] a) E. I. Bagrii, A. I. Nekhaev, A. L. Maksimov, *Pet. Chem.* **2017**, *57*, 183–197; b) E. A. Shokova, V. V. Kovalev, *Russ. J. Org. Chem.* **2012**, *48*, 1007–1040.
- [6] Selected examples: a) M. Larrosa, B. Zonker, J. Volkman, F. Wech, C. Logemann, H. Hausmann, R. Hrdina, *Chem. Eur. J.* **2018**, *24*, 6269–6276; b) H. Fu, P.-X. Shen, J. He, F. Zhang, S. Li, P. Wang, T. Liu, J.-Q. Yu, *Angew. Chem. Int. Ed.* **2017**, *56*, 1873–1876; c) N. Gulia, O. Daugulis, *Angew. Chem. Int. Ed.* **2017**, *56*, 3630–3634; d) M. Larrosa, S. Heiles, J. Becker, B. Spengler, R. Hrdina, *Adv. Synth. Catal.* **2016**, *358*, 2163–2171; e) Z. Fan, S. Shu, J. Ni, Q. Yao, A. Zhang, *ACS Catal.* **2016**, *6*, 769–774; f) Y.-X. Lao, J.-Q. Wu, Y. Chen, S.-S. Zhang, Q. Li, H. Wang, *Org. Chem. Front.* **2015**, *2*, 1374–1378.
- [7] a) S. Rej, Y. Ano, N. Chatani, *Chem. Rev.* **2020**, *120*, 1788–1887; b) R. Hrdina, *Synthesis* **2019**, *51*, 629–642.
- [8] a) T. J. Chow, T.-K. Wu, *J. Org. Chem.* **1991**, *56*, 6833–6835; b) T. J. Chow, T.-K. Wu, *Tetrahedron Lett.* **1989**, *30*, 1279–1280.
- [9] a) T. J. Chow, Y.-S. Chao, L.-K. Liu, *J. Am. Chem. Soc.* **1987**, *109*, 797–804; b) A. P. Marchand, A. D. Earlywine, M. J. Heeg, *J. Org. Chem.* **1986**, *51*, 4096–4100; c) A. P. Marchand, A. D. Earlywine, M. J. Heeg, *J. Org. Chem.* **1986**, *51*, 4096–4100; d) T. J. Chow, L.-K. Liu, Y.-S. Chao, *J. Chem. Soc. Chem. Commun.* **1985**, 700–701; e) A. P. Marchand, A. Wu, *J. Org. Chem.* **1985**, *50*, 396–398; f) T. J. Chow, Y.-S. Chao, *J. Organomet. Chem.* **1985**, *296*, C23–C26.
- [10] a) H. N. Lim, G. Dong, *Org. Lett.* **2016**, *18*, 1104–1107; For the seminal work see: b) T.-A. Mitsudo, T. Suzuki, S.-W. Zhang, D. Imai, K.-I. Fujita, T. Manabe, M. Shiotsuki, Y. Watanabe, K. Wada, T. Kondo, *J. Am. Chem. Soc.* **1999**, *121*, 1839–1850.
- [11] A. Zieliński, X. Marset, C. Golz, L. M. Wolf, M. Alcarazo, *Angew. Chem. Int. Ed.* **2020**, *59*, 23299–23305.
- [12] Deposition numbers 2075609–2075619 contain the supplementary crystallographic data for this paper. These data are provided free of charge by the joint Cambridge Crystallographic Data Centre and Fachinformatizierungs-zentrum Karlsruhe Access Structures service www.ccdc.cam.ac.uk/structures.
- [13] a) T. Agou, N. Wada, K. Fujisawa, T. Hosoya, Y. Mizuhata, N. Tokitoh, H. Fukumoto, T. Kubota, *Inorg. Chem.* **2018**, *57*, 9105–9114; b) R. F. Stockel, *Can. J. Chem.* **1968**, *46*, 2625–2628.
- [14] L. Gu, L. M. Wolf, A. Zieliński, W. Thiel, M. Alcarazo, *J. Am. Chem. Soc.* **2017**, *139*, 4948–4953.
- [15] W. R. Cullen, D. F. Dong, J. A. J. Thompson, *Can. J. Chem.* **1969**, *47*, 4671–4677.
- [16] Reproducible results are only obtained when freshly prepared $\text{NaB}(\text{C}_6\text{F}_5)_4$ is used. Only trace conversions are observed without $\text{NaB}(\text{C}_6\text{F}_5)_4$.
- [17] a) A. P. Marchand, S. Alihodžić, I. N. N. Namboothiri, B. Ganguly, *J. Org. Chem.* **1998**, *63*, 8390–8396; b) I. Tabushi, J. Hamuro, R. Oda, *J. Org. Chem.* **1968**, *33*, 2108–2109.
- [18] a) R.-Y. Zhu, Z.-Q. Li, H. S. Park, C. H. Senanayake, J.-Q. Yu, *J. Am. Chem. Soc.* **2018**, *140*, 3564–3568; b) Y.-Q. Chen, Z. Wang, Y. Wu, S. R. Wisniewski, J. X. Qiao, W. R. Ewing, M. D. Eastgate, J.-Q. Yu, *J. Am. Chem. Soc.* **2018**, *140*, 17884–17894; c) G. Xia, Z. Zhuang, L.-Y. Liu, S. L. Schreiber, B. Melillo, J.-Q. Yu, *Angew. Chem. Int. Ed.* **2020**, *59*, 7783–7787; *Angew. Chem.* **2020**, *132*, 7857–7861.
- [19] D. Shabashov, O. Daugulis, *J. Am. Chem. Soc.* **2010**, *132*, 3965–3972.
- [20] a) H. Cheng, J. Hoffman, P. Le, S. K. Nair, S. Cripps, J. Matthews, C. Smith, M. Yang, S. Kupchinsky, K. Dress, M. Edwards, B. Cole, E. Walters, C. Loh, J. Ermoloeff, A. Fanjul, G. B. Bhat, J. Herrera, T. Pauly, N. Hosea, G. Paderes, P. Rejto, *Bioorg. Med. Chem. Lett.* **2010**, *20*, 2897–2902; b) H. Cheng, C. R. Smith, Y. Wang, T. J. Parrott, K. R. Dress, S. K. Nair, J. E. Hoffman, P. T. Q. Le, S. W. Kupchinsky, Y. Yang, S. J. Cripps, B. Huang, *PCT Int. Appl.* WO 2005108359 A1 **2005**.
- [21] For related Pd-catalyzed $\text{C}(\text{sp}^3)\text{-H}$ alkynylation reactions see: a) V. G. Landge, A. Parveen, A. Nandakumar, E. Balaraman, *Chem. Commun.* **2018**, *54*, 7483–7486; b) Y. Ano, M. Tobisu, N. Chatani, *J. Am. Chem. Soc.* **2011**, *133*, 12984–12986.
- [22] a) A. D. Becke, *Phys. Rev. A* **1988**, *38*, 3098–3100; b) A. D. Becke, *J. Chem. Phys.* **1993**, *98*, 5648–5652.
- [23] a) N. Mandal, A. Datta, *J. Org. Chem.* **2020**, *85*, 13228–13238; b) Y. Li, P. Zhang, Y.-J. Liu, Z.-X. Yu, B.-F. Shi, *ACS Catal.* **2020**, *10*, 8212–8222.
- [24] S. I. Gorelsky, D. Lapointe, K. Fagnou, *J. Am. Chem. Soc.* **2008**, *130*, 10848–10849.

RESEARCH ARTICLE

Towards an Effective Synthesis of Difunctionalized Heptacyclo [6.6.0.0^{2,6}.0^{3,13}.0^{4,11}.0^{5,9}.0^{10,14}]tetradecane: Ligand Effects on the Cage Assembly and Selective C–H Arylation Reactions

Adv. Synth. Catal. **2021**, *363*, 1–9

 X. Marset, M. Recort-Fornals, M. Kpante, A. Zieliński, C. Golz, L. M. Wolf*, M. Alcarazo*



● New phosphines as ancillary ligands

● C-H functionalization of the cage
● Theoretical study on the regioselectivity of the reaction